CHEMISTRY
A EUROPEAN JOURNAL

DOI: 10.1002/chem.200601520

Aminoborylene Complexes of Group 6 Elements and Iron: A Synthetic, Structural, and Quantum Chemical Study

Benoît Blank,[a] Miriam Colling-Hendelkens,[b] Carsten Kollann,[a] Krzysztof Radacki,[a] Daniela Rais,[a] Katharina Uttinger,[a] George R. Whittell,[a] and Holger Braunschweig*[a]

Abstract: Transition-metal–borylene complexes of the type $[(OC)_5M{=}BR]$ {M = Cr, Mo, W; R = $N(SiMe_3)_2$, **1a**–**3a**, $Si(SiMe_3)_3$, **4a**} and $[(OC)_4Fe{=}B{=}N(SiMe_3)_2]$ (**8**) were prepared by salt elimination reactions. Synthesis of the latter complex was accompanied by the formation of substantial amounts of an unusual dinuclear iron complex $[Fe_2\{\mu\text{-}C_2O_2(BN(SiMe_3)_2)\}_2(CO)_6]$ (**9**). The aminoborylene complexes of Group 6 metals were converted to *trans*-$[(Cy_3P)(CO)_4M{=}B{=}N(SiMe_3)_2]$ (**5a**–**7a**) by irradiation in the presence of PCy_3. Structural and spectroscopic parameters were discussed with respect to the *trans*-effect of the borylene ligand and the degree of M–B d_π–p_π-backbonding. Computational studies were performed on Group 6–borylene complexes. The population and topological analyses as well as the molecular orbital composition are consistent with the presence of both σ-and π-type interactions. There are, however, indications that the d_π–p_π-backbonding in the silylborylene complex is significantly more pronounced than in the aminoborylene complexes.

Keywords: boron · chromium · molybdenum · organometallic chemistry · tungsten

Introduction

Transition-metal complexes containing unsaturated carbon-based ligands are of fundamental importance to a wide range of catalytic reactions.[1] In these processes, the C-donating group may serve as either a site of reactivity itself or moderate the electron density at the metal center and merely spectate. For instance, both roles can be found in the $[(H_2IMes)(PCy_3)Cl_2Ru{=}CHPh]$ {H_2IMes = bis(mesityl) imidazol-2-ylidene} catalyzed olefin metathesis reaction,[2] where the benzylidene and N-heterocyclic carbene (NHC) ligands exhibit the respective functions. The different roles adopted by these superficially similar ligands have been attributed to the nature of the C-bound substituents and their influence on the σ-donor and π-acceptor properties.[3] In principle, formally exchanging the NHC ligand for an isolobal species containing the more electropositive element boron would also affect the reactivity of the complex, and possibly in a complementary way. The design of such borylene complexes (**:**BR) for catalytic applications, however, has been hampered by a lack of systematic experimental evidence regarding the effect of the boron-bound substituent on the σ-donor/π-acceptor properties of the ligand. This has, for the main part, been due to the requirement of bulky and/or π-donating groups {for example, Cp* [= η^5-C_5Me_5], $N(SiMe_3)_2$, $Si(SiMe_3)_3$ and Mes} in this position to achieve isolable compounds.[4] Furthermore, it has been shown that an appropriate choice of transition metal–ligand fragment is also required for stability.[4] As a result of these factors, $[(OC)_3CpV{=}B{=}N(SiMe_3)_2]$,[5] $[(OC)_5M{=}B{=}N(SiMe_3)_2]$ (M = Cr, W),[6] $[(OC)_5Cr{=}B{-}Si(SiMe_3)_3]$,[7] $[(OC)_2Cp^*Fe{=}BMes)]^+$,[8] $[(OC)_2Cp^*Fe{=}B{=}N(iPr)_2)]^+$,[9] $[(OC)_2Cp^*Fe{=}B{=}N(Cy)_2)]^+$,[10] and $[(OC)_2Cp^*Fe{-}B{=}M(CO)_n]$ (M = Fe, n = 4; M = Cr, n = 5)[11] represent the only fully characterized, terminal borylene complexes with two-coordinated boron to have been reported to date.

The scarcity of borylene complexes in the literature has not prevented the nature of the metal–boron bond being probed on a theoretical level by a number of groups. In fact,

[a] B. Blank, Dr. C. Kollann, Dr. K. Radacki, Dr. D. Rais, K. Uttinger, Dr. G. R. Whittell, Prof. Dr. H. Braunschweig
Institut für Anorganische Chemie
Bayerische Julius-Maximilians-Universität Würzburg
Am Hubland, 97074 Würzburg (Germany)
Fax: (+49)-931-888-4623
E-mail: h.braunschweig@mail.uni-wuerzburg.de

[b] Dr. M. Colling-Hendelkens
Institut für Anorganische Chemie der Technischen Hochschule
Templergraben 55, 52056 Aachen (Germany)

Supporting information for this article is available on the WWW under http://www.chemeurj.org/ or from the author.

initial studies appeared prior a first realization of such a complex and focused the coordination properties of BF, BNH_2 and BO^- relative to other terminally ligated, isoelectronic diatomic molecules of the second period, such as N_2 and more notably CO.[12] These results indicated that both BF and BNH_2 should be better σ-donors and π-acceptors than CO, leading to higher bond dissociation energies for M–B with respect to M–C. It was also noted, that ligation would result in a build-up of positive charge at boron and that this coupled with the small HOMO–LUMO gap of these ligands may result in kinetic instability. The authors suggested that this issue might be addressed by protecting the frontier orbitals of the borylene fragment with bulky substituents at nitrogen. To this aim they additionally studied both the terminal and bridging coordination of $BNMe_2$,[12b] the latter of which had only recently been realized experimentally.[13]

The preparation of the first complexes to contain terminally ligated borylene ligands in 1998[6a] and the somewhat controversial report of a "ferrogallyne"[14] resulted in renewed interest in complexes containing transition-metal–Group 13 bonds. The theoretical emphasis was now the investigation of how the choice of element (E), the associated substituent (R) and the other ligands (L) affected the nature of the transition-metal–element bond (L_nM–ER).[15] In general, this work concluded that the interaction was predominantly ionic, with the major contribution to the covalent component arising from σ-donation. It was also noted that the contribution from π-backdonation increased as the π-basicity and π-acidity of R and L, respectively, decreased. With respect to Group 13 as a whole, it was found that the ionic contribution and both the σ- and π-components of the orbital contribution to bonding were larger for boron than any other element.

We herein report the syntheses of $[(OC)_5M{=}B{=}N(SiMe_3)_2]$ (M = Cr, Mo, W) and $[(OC)_5Cr{=}B{-}Si(SiMe_3)_3]$ by a salt-elimination methodology, which to date has proven the only route to prepare neutral terminal borylene complexes for a range of transition metals and boron-based substituents. Furthermore, the aminoborylene complexes were successfully converted into corresponding phosphine complexes of the type *trans*-$[(Cy_3P)(OC)_4M{=}B{=}N(SiMe_3)_2]$. This is complemented by full spectroscopic and structural characterization and a comparison of this data with the results of a DFT study on corresponding model compounds. The work thus constitutes the first tandem synthetic–theoretical study of its kind on terminal borylene complexes. In addition, we elaborate on the synthesis of $[(OC)_4Fe{=}B{=}N(SiMe_3)_2]$ and discuss the formation and structure of $[Fe_2\{\mu\text{-}C_2O_2(BN(SiMe_3)_2)\}_2(CO)_6]$ via a competing reaction pathway.

Abstract in German: *Übergangsmetallborylenkomplexe des Typs $[(OC)_5M{=}BR]$ {M = Cr, Mo, W; R = $N(SiMe_3)_2$, **1a–3a**, $Si(SiMe_3)_3$, **4a**} und $[(OC)_4Fe{=}B{=}N(SiMe_3)_2]$ (**8**) konnten über den Weg der Salzeliminierung dargestellt werden. Bei letzterer Reaktion fielen nicht vernachlässigbare Mengen des ungewöhnlichen zweikernigen Eisenkomplexes $[Fe_2\{\mu\text{-}C_2O_2(BN(SiMe_3)_2)\}_2(CO)_6]$ (**9**) an. Unter photolytischen Bedingungen in Gegenwart von PCy_3 wurden die Aminoborylenkomplexe der Gruppe 6 zu den Phosphan-substituierten Komplexen* trans-$[(Cy_3P)(CO)_4M{=}B{=}N(SiMe_3)_2]$ *(**5a–7a**) umgesetzt. Die strukturellen und spektroskopischen Parameter wurden in Bezug auf den* trans-*Effekt des Borylenliganden und den Grad der M–B d_π–p_π-Rückbindung diskutiert. Außerdem wurden theoretische Berechnungen zu den Borylenkomplexen der Gruppe 6 durchgeführt. Die Populations- und topologischen Analysen, sowie die Molekülorbitalzusammensetzungen stehen im Einklang mit der gleichzeitigen Anwesenheit von σ- und π-artigen Wechselwirkungen. Es gibt jedoch Anzeichen, dass die d_π–p_π-Rückbindung im Silylborylenkomplex deutlich ausgeprägter ist als in den Aminoborylenkomplexen.*

Results and Discussion

Characterization of terminal Group 6–borylene complexes $[(OC)_5M{=}B{=}N(SiMe_3)_2]$ (M = Cr, 1a; Mo, 2a; W, 3a): The terminal borylene complexes $[(OC)_5M{=}B{=}N(SiMe_3)_2]$ (M = Cr, **1a**;[6] Mo, **2a**; W, **3a**[6a]) were obtained by salt-elimination reactions of the corresponding dianions $Na_2[M(CO)_5]$ and the dichloroborane $Cl_2BN(SiMe_3)_2$. All compounds were isolated after recrystallization from hexanes as pale yellow or colorless, analytically pure solids in yields between 32 and 56%. The aminoborylene complexes proved to be only moderately air- and moisture sensitive and stable in solution and in the solid state over prolonged periods of time. In solution the compounds were characterized by multinuclear NMR techniques and display a sharp singlet in the ^1H NMR spectrum (**1a**: $\delta = 0.14$; **2a**: $\delta = 0.15$; **3a**: $\delta = 0.12$ ppm) for the chemically equivalent $SiMe_3$ groups and the expected deshielded signals for the metal bound boron atom in the $^{11}B\{^1H\}$ NMR spectra (**1a**: $\delta = 92.3$; **2a**: $\delta = 89.7$; **3a**: $\delta = 86.6$ ppm). The axial and the four equatorial CO ligands at each metal center give rise to two signals in the $^{13}C\{^1H\}$ NMR spectra {**1a**: $\delta = 218.0$ (CO_{ax}), 217.6 (CO_{eq}); **2a**: $\delta = 206.8$ (CO_{ax}), 207.7 (CO_{eq}); **3a**: $\delta = 196.5$ (CO_{ax}), 197.2 ppm (CO_{eq})}.

Single crystals suitable for X-ray diffraction studies were obtained for all three aminoborylene complexes from hexanes at low temperatures. The three compounds are isostructural and crystallize in the space group $P\bar{1}$. They display a central M-B-N moiety, the structure of which is very close to linear {**1a**: Cr-B-N = 177.4(4); **2a**: Mo-B-N = 177.81(11); **3a**: W-B-N = 177.9(5)°}, and short B–N distances {**1a**: 1.353(6); **2a**: 1.3549(18); **3a**: 1.338(8) Å}, which, together with the trigonal-planar geometry of the nitrogen atoms, prove the presence of B=N double bonds. A comparison of the M–B distances {**1a**: Cr–B = 1.996(6); **2a**: Mo–B = 2.1519(15); **3a**: W–B = 2.151(7) Å} confirms the trend expected from the different covalent radii of the Group 6

metals. The overall geometry of the M-B-N moiety in **1a–3a** resembles that of the only other structurally characterized terminal aminoborylene complex $[(\eta^5\text{-}C_5H_5)(OC)_3V{=}B{=}N(SiMe_3)_2]$,[5] and corresponds, together with the spectroscopic data and in agreement with earlier DFT studies,[12,15] to the description of a metal–boron double bond consisting of a strong B−M σ-donation and a somewhat weaker M−B π-backdonation (**2a**: Figure 1).

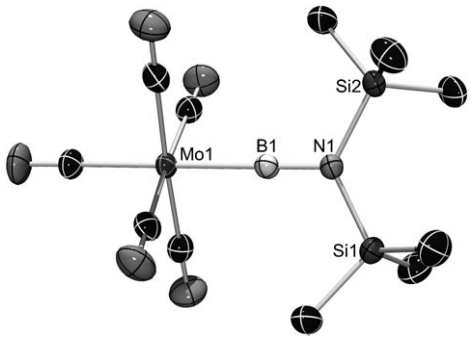

Figure 1. Molecular structure of $[(OC)_5Mo{=}B{=}N(SiMe_3)_2]$ (**2a**).

$[(OC)_5Cr{=}B{-}Si(SiMe_3)_3]$ (4a): Analogous to the preparation of **1a–3a** the reaction of $Na_2[Cr(CO)_5]$ with $Cl_2BSi(SiMe_3)_3$ furnished the silylborylene complex $[(OC)_5Cr{=}B{-}Si(SiMe_3)_3]$ (**4a**) as pale yellow crystals in 81% yield. The boron bound bulky hypersilyl substituent provides greater steric protection than the aforementioned $N(SiMe_3)_2$ group, but lacks the potential of ligand-to-boron π-stabilization, thus rendering the metal-coordinated borylene center coordinatively and electronically unsaturated. This particular bonding situation strongly affects the properties of the silylborylene complex, and is for example responsible for the significantly decreased stability of **4a** with respect to **1a–3a**. Even in the solid state the product proved to be extremely air and moisture sensitive and underwent rapid decomposition in solution at ambient temperature. While ^1H NMR ($\delta = 0.34$ ppm) and $^{13}C\{^1H\}$ NMR spectra ($\delta = 213.3$ ppm, CO_{eq} and CO_{ax}) are rather similar to the data obtained for **1a–3a**, the $^{11}B\{^1H\}$ NMR signal at $\delta = 204.3$ ppm again emphasizes the particular situation of the borylene center. This resonance is extremely deshielded, even with respect to the signals of the aforementioned aminoborylene complexes, and reflects the exchange of the electronegative, π-stabilizing amino group[16] for the hypersilyl ligand, reminiscent of the markedly different $^{11}B\{^1H\}$ NMR resonances observed for the borylene bridged dinuclear manganese complexes $[(\mu\text{-}BR)\{(\eta^5\text{-}C_5H_5)Mn(CO)_2\}_2]$ (R = NMe_2, $\delta = 103$; R = *t*Bu, $\delta = 170$ ppm).[13,17] It should be noted that similarly deshielded boron resonances are known for interstitial boron atoms in metal clusters,[18] but have only very recently been reported for boron in a classical bonding situation namely in the case of the metalloborylene complexes $[(OC)_2Cp^*Fe{-}B{=}Cr(CO)_5]$ ($\delta = 204.6$) and $[(OC)_2Cp^*Fe{-}B{=}Fe(CO)_4]$ ($\delta = 190.9$ ppm).[11,19]

An X-ray diffraction study was performed on single crystals of **4a** obtained from a hexane solution at −78 °C (see Figure 2).

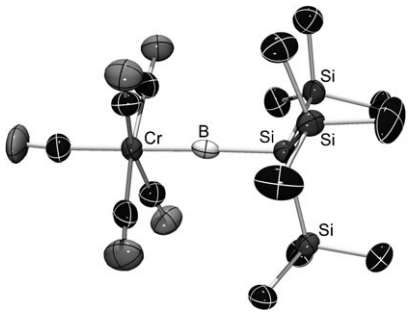

Figure 2. Molecular structure of $[(OC)_5Cr{=}BSi(SiMe_3)_3]$ (**4a**).

The molecule crystallizes in the space group $P3_2$ and adopts C_1 symmetry. While the approximate linearity of the central Cr-B-Si moiety (176.9(5)°) resembles that of the respective M-B-N units in **1a–3a**, further pertinent structural parameters associated with the $BM(CO)_5$ fragments are markedly different. In particular, the B−Cr distance in **4a** (1.878(10) Å) is about 0.12 Å smaller than that in the amino counterpart **1a**. Furthermore, inspection of the M−CO distances and angles reveals that: i) the $Cr{-}C_{ax}$ bond (1.939(10) Å) in **4a** exceeds that in **1a** (1.908(6)), ii) the $Cr{-}C_{eq}$ distances (average 1.894 Å) in **4a** are almost 0.05 Å smaller than the $Cr{-}C_{ax}$ distances while corresponding distances in **1a–3a** vary only slightly, and iii) that the equatorial CO ligands in **4a** express the strongest umbrella effect (**4a**: B-Cr-C_{eq} = 85, Cr-C_{eq}-O = 176; **1a**: B-Cr-C_{eq} = 88, Cr-C_{eq}-O = 179; **2a**: Mo-C_{eq}-O = 179, B-Mo-C_{eq} = 88; **3a**: B-W-C_{eq} = 89, W-C_{eq}-O = 179°) of all four compounds.[15c] Hence, all structural data strongly support the presence of increased M−B π-backdonation in **4a** with respect to the terminal aminoborylene complexes, obviously imposed by the lack of π-stabilization provided by the boron bound substituent in the former.

In addition to the aforementioned syntheses of **1a–3a** a variety of reactions between dianionic carbonylates and dihaloboranes were studied in order to broaden the scope of terminal borylene complexes. Surprisingly, however, none of these attempts, in particular reactions of $Na_2[M(CO)_5]$ (M = Mo, W) with $Cl_2BSi(SiMe_3)_3$, were met with success. Only the addition of $Cl_2BGe(SiMe_3)_3$, which had already proven to be a suitable precursor for chloro(germyl)boryl complexes,[20] to a suspension of $Na_2[Cr(CO)_5]$ in toluene at −78 °C yielded the corresponding borylene complex $[(OC)_5Cr{=}B{-}Ge(SiMe_3)_3]$ as indicated by multinuclear NMR spectroscopy (^1H NMR, $\delta = 0.34$; $^{11}B\{^1H\}$ NMR, $\delta = 203.1$ ppm). The oily consistency of the crude product and its pronounced thermolability, however, precluded its isolation in pure form.

Synthesis and characterization of phosphine substituted borylene complexes *trans*-[(Cy$_3$P)(OC)$_4$M=B=N(SiMe$_3$)$_2$] (M = Cr, 5a; Mo, 6a; W, 7a): While preliminary results on the reactivity of the borylene center in terminal borylene complexes have recently been reported,[5,6b,21] corresponding studies on the metal centered reactivity in such complexes, in particular with respect to co-ligand substitution, were not performed. It should be noted though, that our recent investigations on semibridging borylene complexes of the type [(OC)$_4$M(μ-CO){μ-BN(SiMe$_3$)$_2$}M′(PCy$_3$)] (M = Cr, W; M′ = Pd, Pt)[22] led to the structural characterization of *trans*-[(Cy$_3$P)(OC)$_4$Cr=B=N(SiMe$_3$)$_2$] (**5a**), which was isolated in low yields as a one of the products stemming from the degradation of [(OC)$_4$Cr(μ-CO){μ-BN(SiMe$_3$)$_2$}Pd(PCy$_3$)] under thermal or photolytic conditions.

In order to explore the reactivity of [(OC)$_5$M=B=N(SiMe$_3$)$_2$] (M = Cr, Mo, W; **1a–3a**) towards controlled CO-exchange reactions, the aminoborylene complexes were photolyzed in the presence of one equivalent of PCy$_3$. After 4 h, multinuclear NMR spectra indicated the formation of a new product in each reaction mixture with concomitant consumption of the starting materials. In the ^{31}P{^{1}H} NMR spectra a new signal arose at δ = 64.7 (**5a**), 51.1 (**6a**) and 35.0 ppm (**7a**), and in the ^{1}H NMR spectra at approximately δ 0.38 ppm for all three new complexes. The ^{11}B{^{1}H} NMR spectra showed broad signals at δ = 94 (**5a**), 92 (**6a**) and 90 ppm (**7a**), which are slightly downfield shifted with respect to those of the starting borylene complexes **1a–3a**. The presence of only one doublet ($^2J_{P,C}$ = 7–13 Hz) in the carbonyl region of the ^{13}C{^{1}H} NMR spectra indicates the substitution of the carbonyl group *trans*-disposed to the borylene by PCy$_3$ (Scheme 1). All spectroscopic data of the new

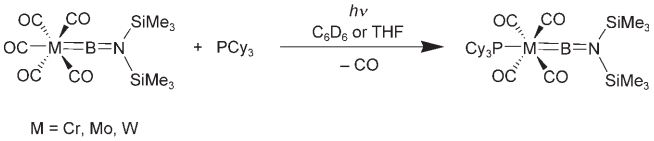

Scheme 1. Formation of the phosphine substituted borylene complexes **5a–7a**.

compounds are consistent with the formulation of phosphine substituted borylene complexes of the type *trans*-[(Cy$_3$P)(OC)$_4$M=B=N(SiMe$_3$)$_2$] (M = Cr, Mo, W; **5a–7a**). The observed selectivity of the ligand exchange may be partially attributed to steric constraints imposed by the bulky cyclohexyl and SiMe$_3$ groups, but provides also evidence for a certain *trans*-influence of the borylene ligand (see below).

In addition to the previously described structure of **5a** in the crystal,[22b] the constitution of the new compounds **6a** and **7a** could be determined by performing single crystal X-ray diffraction studies (Figure 3). Suitable crystals of the compounds *trans*-[(Cy$_3$P)(OC)$_4$M=B=N(SiMe$_3$)$_2$] (M = Mo, **6a**; W, **7a**) were obtained from hexane at −30 °C.

Complex **5a** crystallizes in the monoclinic space group $P2_1/c$, **6a** and **7a** in the triclinic $P\bar{1}$. The P-M-B and the M-

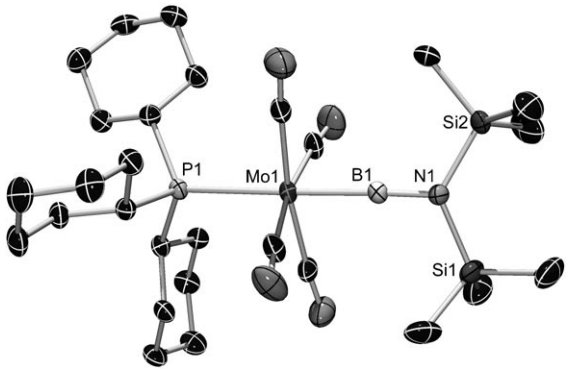

Figure 3. Molecular structure of *trans*-[(Cy$_3$P)(OC)$_4$Mo=B=N(SiMe$_3$)$_2$] (**6a**). Compound **6a** is isostructural to *trans*-[(Cy$_3$P)(OC)$_4$W=B=N-(SiMe$_3$)$_2$] (**7a**).

B-N moieties adopt an almost linear arrangement {P1-Cr1-B1 = 177.87(6), Cr1-B1-N1 = 175.91(16); P1-Mo1-B1 = 178.80(8), Mo1-B1-N1 = 175.3(2); P1-W1-B1 = 178.29(15), W1-B1-N1 = 175.8(5)°}. The B1−N1 distances {**5a**: 1.364(3); **6a**: 1.365(3); **7a**: 1.378(7) Å} are negligibly elongated with respect to the B1−N1 bonds of the starting materials {**1a**: 1.353(6); **2a**: 1.3549(18); **3a**: 1.338(8) Å}, however the M−B1 bond lengths {**5a**: 1.915(2); **6a**: 2.059(3); **7a**: 2.058(6) Å} are shortened by about 9 pm {**1a**: 1.996(6); **2a**: 2.1519(15); **3a**: 2.151(7) Å}. This fact can be understood, when considering the different electronic situation in the two types of complexes, with the fact that the phosphine ligand is a good σ-donor, but a less effective π-acceptor relative to the carbonyl ligand in the unsubstituted borylene complexes. The phosphine allows for a stronger π-backdonation from the metal to the boron atom, hence resulting in a shorter metal−boron bond. The strong metal−boron M→B π-backbonding is also responsible for a more pronounced umbrella effect[7,15c] in **5a–7a** than in the unsubstituted borylenes **1a–3a**. The latter is expressed by the mean values of the B-M-C$_{eq}$ and M-C$_{eq}$-O angles, which are smaller for **5a–7a** than for **1a–3a** {**5a**: B1-Cr1-C(1,3) = 79, Cr1-C(1,3)-O-(1,3) = 174; **1a**: B-Cr-C$_{eq}$ = 88, Cr-C$_{eq}$-O = 179; **6a**: B1-Mo1-C = 86, Mo1-C-O = 175; **2a**: B1-Mo1-C$_{eq}$ = 88, Mo1-C$_{eq}$-O = 179; **7a**: B1-W1-C = 86, W1-C-O = 175; **3a**: B1-W1-C$_{eq}$ = 89, W1-C$_{eq}$-O = 179°}. It should be noted that in **5a** the Si$_2$NB plane is only slightly twisted towards the C2-Cr1-C4-plane (Si1-N1-Cr1-C2 = 11.46, Si2-N1-Cr1-C4 = −1.99°), meaning the planes are almost coplanar and therefore a bending of the carbonyl ligands C2−O2 and C4−O4 towards the [Cr=B=N(SiMe$_3$)$_2$] fragment is precluded for steric reasons {B1-Cr1-C(2,4) = 92, Cr1-C(2,4)-O(2,4) = 178°}. In case of the molybdenum and tungsten complexes **6a** and **7a**, the Si$_2$NB planes lay between the C1-M1-C3 and C2-M1-C4 planes (Si1-N1-Mo1-C3 = 62.54, Si2-N1-Mo1-C2 = 40.30, Si1-N1-W1-C2 = 62.96, Si2-N1-W1-C3 = 39.91°), therefore the umbrella effect affects all the CO groups.

Fe Complexes: The reaction between Na$_2$[Fe(CO)$_4$] and Br$_2$BN(SiMe$_3$)$_2$ was attempted with the view to preparing a

corresponding iron–aminoborylene complex. In contrast to the situation with the Group 6 metal–carbonylates, the reaction with $Na_2[Fe(CO)_4]$ required three days for the borane to be consumed, as indicated by the disappearance of the signal at $\delta = 31.2$ ppm from the $^{11}B\{^1H\}$ NMR spectrum. The longer time-frame for this reaction is presumably due to the poorer solubility of $Na_2[Fe(CO)_4]$ in toluene, relative to $Na_2[M(CO)_5]$ (M = Cr, Mo and W). It is noteworthy that the reaction did not proceed to any appreciable extent over three days when performed in hexane. Another difference between the reactions with iron and those with the Group 6 metals was the selectivity. When the latter processes were monitored by $^{11}B\{^1H\}$ NMR spectroscopy, no products other than the aminoborylene complexes could be observed, whereas two new resonances were observed in the case of the former. The low-field signal ($\delta = 87.3$ ppm) is comparable in frequency to those reported for **1a–3a**, and thus consistent with assignment to the corresponding iron–aminoborylene complex, $[(OC)_4Fe{=}B{=}N(SiMe_3)_2]$ (**8**). Indeed, we previously reported these data[6a] to bring into question the identity of a compound formulated as $[(OC)_4Fe{=}B{=}NMe_2]$, but which exhibited a significantly high-field shifted $^{11}B\{^1H\}$ NMR resonance. The high-field signal ($\delta = 27.3$ ppm) integrated to approximately three-quarters the area of that arising from **8**.

An attempt to isolate **8** by recrystallization of the crude reaction mixture from hexane afforded a crop of yellow crystals, one of which was suitable for study by single crystal X-ray diffraction. The crystals were composed of the novel ferracyclopentadiene complex, $[Fe_2\{\mu\text{-}C_2O_2(BN(SiMe_3)_2)\}_2(CO)_6]$ (**9**) (Figure 4), the structure of which will be discussed later. Given that the formation of **9** is superstoichiometric with respect to CO, the reaction was repeated under an atmosphere of CO in an attempt to increase selectivity for this compound. Somewhat surprisingly, however, the presence of further CO seemed to have the reverse effect, increasing the relative amount of aminoborylene **8** in the reaction mixture. This result would suggest that the extra CO required to form **9** does not arise from carbonyl dissociation from **8**, which might be expected given the high *trans* influence of the borylene ligand.[4] Compound **8** could only be isolated as a moderately impure brown oil. Although a tentative assignment of the NMR and IR data has been made (see Experimental Section), we lack the confidence to draw further conclusions from these results.

We have previously reported that the monoanionic Group 6 transition metal complexes, $K[(\eta^5\text{-}C_5H_5)M(CO)_3]$ (M = Mo and W), react with half an equivalent of $1,2\text{-}B_2(NMe_2)_2I_2$ to afford the boryloxycarbyne complexes, $[\{(\eta^5\text{-}C_5H_5)(OC)_2M{\equiv}CO\}_2B_2(NMe_2)_2]$ (M = Mo and W), under kinetic control.[23] This result clearly demonstrates that when the electrophile is sufficiently large and oxophilic, then attack at a carbonyl oxygen can become preferential. Indeed, when the smaller dichloro or dibromo analogues are employed, electrophilic attack occurs at the metal center to afford the diborane(4)yl complexes, $[(\eta^5\text{-}C_5H_5)M\{B(NMe_2)B(NMe_2)X\}(CO)_2]$ (M = Mo and W; X = Cl and Br).[24] Compounds of this type are also the thermodynamic products of the reactions involving $1,2\text{-}B_2(NMe_2)_2I_2$, with the boryloxycarbyne complexes undergoing a thermal rearrangement to the mixed boryloxycarbyne-diborane(4)yl compounds, $[\{(\eta^5\text{-}C_5H_5)(OC)_2M{\equiv}CO\}B(NMe_2)B(NMe_2)\{M(CO)_3(\eta^5\text{-}C_5H_5)\}]$ (M = Mo, W).[23] It can therefore be envisaged that electrophilic attack at the carbonyl oxygen may, in part, occur with the dianion, $[Fe(CO)_4]^{2-}$, thus leading to the observed product mixture. Although a discussion of the reaction mechanism is complicated by the ill-defined reaction stoichiometry, the intermediacy of a bis(boryloxycarbyne) complex appears plausible (Scheme 2). Comparable reactivity has been previously observed for $Na_2[Fe(CO)_4]$ with the similarly hard electrophile, Me_3SiBr, to yield the analogous ferracyclopentadiene, $[Fe_2\{\mu\text{-}C_2O_2(SiMe_3)_2\}_2(CO)_6]$.[25] The reaction of $[Fe(CO)_4]^{2-}$ with $Cl_2BN(SiMe_3)_2$, in the absence of additional CO, afforded **9** as the only product and enabled subsequent isolation and confirmation that it was indeed this species that gave rise to the initially observed $^{11}B\{^1H\}$ NMR resonance at $\delta = 27.3$ ppm.

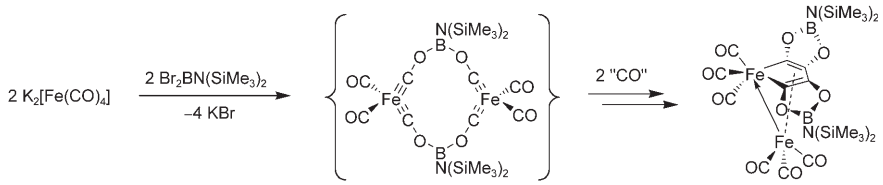

Scheme 2. Possible mechanism for the formation of $[Fe_2\{\mu\text{-}C_2O_2(BN(SiMe_3)_2)\}_2(CO)_6]$ (**9**).

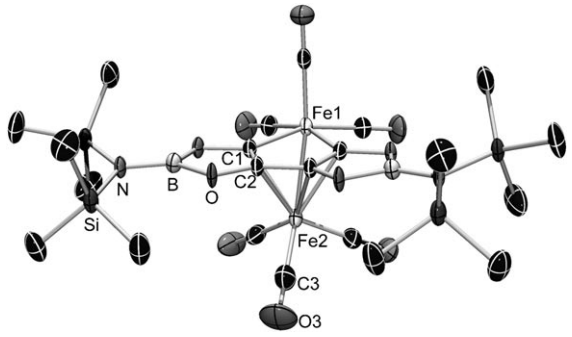

Figure 4. Molecular structure of $[Fe_2\{\mu\text{-}C_2O_2(BN(SiMe_3)_2)\}_2(CO)_6]$ (**9**).

The ^1H NMR spectrum of **9** exhibited two resonances ($\delta = 0.23$ and 0.25 ppm) at chemical shifts characteristic of methyl groups bound to silicon. The presence of two such signals results from hindered rotation about the B=N double bond, which renders the two methyl groups on nitrogen chemically inequivalent. This inequivalence is also apparent in the $^{13}C\{^1H\}$ spectrum, where two resonances are also observed for the methyl substituents ($\delta = 3.4$ and 4.0 ppm). In

addition, two resonances are observed for both metallacyclic ring carbons ($\delta = 129.8$ and 182.9 ppm) and the iron-bound carbonyl ligands ($\delta = 210.1$ and 211.2 ppm). The former is consistent with the crystallographic symmetry (see below) while the latter suggests that the rate of exchange of the three carbonyl ligands per iron center is rapid on the NMR time scale. In the $^{11}B\{^1H\}$ NMR spectrum, the frequency of the single resonance observed is in the range of what would be expected for a three-coordinate boron center bound to three π-donating substituents.[26] The IR spectrum exhibits four bands ($\tilde{\nu}$ = 2078, 2036, 2012 and 1995 cm^{-1}) at frequencies characteristic of terminal carbonyl ligands.[27] The number and positions of these bands are comparable to those of other well-characterized ferracyclopentadienes.[28]

Compound **9** crystallized in the monoclinic space group $P2_1/m$ with the crystallographic mirror plane containing both iron centers and bisecting the metallacyclic ring (Figure 4). Each iron atom exhibits a pseudooctahedral coordination geometry with a facial arrangement of the three carbonyl ligands. When viewed along the Fe–Fe vector, these two groups of carbonyl ligands effectively eclipse one another with the molecule adopting the so-called "sawhorse" configuration.[29] Consistent with this assignment is the absence of a semibridging carbonyl ligand, as evidenced by the most acute Fe-C-O bond angle {Fe1-C3-O3 = 176.2(5)°} deviating little from linearity. This configuration is much less common than the "non-sawhorse",[29] and presumably owes its existence to the presence of four electron-withdrawing oxide substituents on the metallacyclic ring. These help to relieve the increased electron density at the ring iron atom that arises from the formally dative Fe–Fe bond and thus eliminate the need for this to be achieved via a semibridging carbonyl ligand. The ring iron atom forms two formal σ-bonds to the adjacent carbon centers {Fe1–C1 = 1.926(4) Å}, the length of which fall in the range observed for other ferracyclopentadienes.[28,29] Similarly, the formal C=C double {C1–C2 = 1.398(5) Å} and single bonds {C2–C2′ = 1.410(6) Å} have lengths typical for this class of compound.[29] The tendency of these two distances to converge arises from the interaction of the η^5-bound $Fe(CO)_3$ fragment with the π_3* orbital of the butadiene moiety.[30] Thus, Fe2 interacts with the ring via two π-bonds {Fe2–C1 = 2.140(4) and Fe2–C2 = 2.146(4) Å}, in addition to the formally dative Fe–Fe bond {2.533(2) Å}. The lengths of these interactions are comparable to those observed for other "sawhorse" ferracyclopentadiene complexes.[29]

Calculations: All SCF computations reported herein were carried out using the Gaussian03 package running on a cluster of Linux workstations.[31] Calculations were performed using DFT methods, applying the three hybrid functional B3LYP[32–34] using 6-31G(d,p) basis functions sets for nonmetals and Wachters+f (Cr only) or Stuttgart relativistic, small core ECP basis sets for metals.[35] The results for all computed chromium complexes were very similar in both basis, therefore we reported only the results computed with Stuttgart RSC bases, because it was the aim to compare Cr with its higher congeners. Vibrational analyses for all stationary points were carried out analytically.[36] NMR chemical shifts calculated with GIAO method were adjusted to TMS or diborane(6) and recalculated to the standard $BF_3{\cdot}Et_2O$ scale. The Electron Localization Function was computed with the TopMoD package.[37] The charges given in the text are Natural Population Analysis charges obtained with the NBO 5 program.[38] Charge Decomposition Analysis was calculated with the CDA 2.1 program.[39] Illustrations of ELF and orbitals were prepared with Molekel 4.3.[40] The total energies E_h and the ZPVE are given in the Supporting Information.

The DFT calculations were carried out for compounds **1a**–**4a** as well as for the model molecules with SiH_3 or H substituents. In the case of **5a** $N(SiMe_3)_2$ was modeled with $N(SiH_3)_2$ and the bulky tricyclohexylphosphine was replaced by PMe_3 (**5b**) or PH_3 (**5c**). The molecular structures of all computed molecules were obtained by complete geometry optimization—the parent molecules (**1**–**3c**) in C_{2v} or C_s (**4c**) and all others in C_1 symmetry. Vibrational analyses for all optimized geometries demonstrated that they are all energy minima at B3LYP level.

Comparison of calculated and experimental values of structural and spectroscopic parameters: Salient geometrical parameters of the experimental and computed borylene complexes are summarized in Table 1. The interatomic distances are mostly overestimated by 1–3 pm, which can be expected from the comparison of solid-state and gas-phase species and was observed earlier for computations on this level of theory.[5,7,15h] The worst agreement is observed between the Cy_3P-substituted chromium borylene complex **5a** and model compounds **5b**,**c** as a result of the influence of the bulky phosphine ligand. A comparison of the calculated structural parameters in **1**–**4** shows, that geometries around the transition metal are generally only slightly affected by the bulkiness of organic substituents. However, decreasing the size of the organic groups (**a**–**c**), causes a systematic shortening of the M–B bond, which can be explained by steric interactions. As one can expect, a shorter B–M bond leads to a stronger overlap between both atoms, and results in weaker M–CO interactions between the metal atom and the carbonyl ligands, that is, the M–C bond lengths increase. This effect is less pronounced when chromium is replaced by its heavier congeners, as Mo and W impose a longer M–B distance.

Experimental and calculated spectroscopic data for the terminal borylene complexes are presented in Table 2. The IR stretching frequencies of the carbonyl groups are generally well reproduced, in particular, when the model ligands are extended from H and SiH_3 to $SiMe_3$. The most pronounced difference between the IR spectra of **1a**–**3a** and **4a** is the presence of a fourth (1982 cm^{-1}), very weak B_1 stretching in **4a**. For the C_{4v}-symmetric $(OC)_5M$ fragment three vibrations have to be expected. The introduction of a bulky tris(trimethylsilyl) group in **4a** decreases the symmetry of the molecule (see Table 1), increases the umbrella

Table 1. Selected experimental and calculated (in italics) structural data of $[(OC)_5M{=}B{=}NR_2]$ (M = Cr, Mo, W, **1–3**; R = $SiMe_3$, SiH_3, H, **a–c**), $[(OC)_5Cr{=}B\text{-}SiR_3]$ (R = $SiMe_3$, SiH_3, H; **4a–c**), $[(R'_3P)(OC)_4Cr{=}B{=}NR_2]$ (R = $SiMe_3$, R′ = Cy, **5a**; R = SiH_3, R′ = Me, **5b**; R = R′ = H, **5c**) and $[(Cy_3P)(OC)_4M{=}B{=}N(SiMe_3)_2]$ (M = Mo, **6a**; W, **7a**).

		B–N/Si [Å]	M–B [Å]	M–L_{ax} [Å]	M–C_{eq} [Å][a]	M-B-N/Si [°]
$[(OC)_5Cr{=}B{=}N(SiMe_3)_2]$	(**1a**)	1.353(6)	1.996(6)	1.908(6)	1.890	177.4(4)
		1.362	*1.983*	*1.910*	*1.895*	*180.0*
$[(OC)_5Cr{=}B{=}N(SiH_3)_2]$	(**1b**)	*1.372*	*1.950*	*1.919*	*1.900*	*180.0*
$[(OC)_5Cr{=}B{=}NH_2]$	(**1c**)	*1.373*	*1.944*	*1.937*	*1.911*	*180.0*
$[(OC)_5Mo{=}B{=}N(SiMe_3)_2]$	(**2a**)	1.355(2)	2.152(2)	2.075(2)	2.056	177.81(11)
		1.361	*2.148*	*2.083*	*2.059*	*180.0*
$[(OC)_5Mo{=}B{=}N(SiH_3)_2]$	(**2b**)	*1.373*	*2.116*	*2.094*	*2.063*	*180.0*
$[(OC)_5Mo{=}B{=}NH_2]$	(**2c**)	*1.373*	*2.102*	*2.100*	*2.064*	*180.0*
$[(OC)_5W{=}B{=}N(SiMe_3)_2]$	(**3a**)	1.338(8)	2.151(7)	2.040(6)	2.035	177.9(5)
		1.361	*2.168*	*2.087*	*2.069*	*180.0*
$[(OC)_5W{=}B{=}N(SiH_3)_2]$	(**3b**)	*1.372*	*2.139*	*2.097*	*2.073*	*180.0*
$[(OC)_5W{=}B{=}NH_2]$	(**3c**)	*1.373*	*2.126*	*2.102*	*2.074*	*180.0*
$[(OC)_5Cr{=}B{-}Si(SiMe_3)_3]$	(**4a**)	1.998(10)	1.878(10)	1.939(10)	1.894	176.9(5)
		1.999	*1.906*	*1.948*	*1.899*	*177.1*
$[(OC)_5Cr{=}B{-}Si(SiH_3)_3]$	(**4b**)	*2.010*	*1.882*	*1.961*	*1.905*	*178.5*
$[(OC)_5Cr{=}B{-}SiH_3]$	(**4c**)	*2.027*	*1.871*	*1.967*	*1.907*	*179.8*
$[(Cy_3P)(OC)_4Cr{=}B{=}N(SiMe_3)_2]$	(**5a**)	1.364(3)	1.915(2)	2.4159(5)	1.8695	175.91(16)
$[(Me_3P)(OC)_4Cr{=}B{=}N(SiH_3)_2]$	(**5b**)	*1.386*	*1.903*	*2.397*	*1.887*	*179.6*
$[(H_3P)(OC)_4Cr{=}B{=}N(SiH_3)_2]$	(**5c**)	*1.382*	*1.905*	*2.377*	*1.892*	*179.9*
$[(Cy_3P)(OC)_4Mo{=}B{=}N(SiMe_3)_2]$	(**6a**)	1.365(3)	2.059(3)	2.6003(7)	2.0365	175.3(2)
$[(Cy_3P)(OC)_4W{=}B{=}N(SiMe_3)_2]$	(**7a**)	1.378(7)	2.058(6)	2.572(1)	2.0268	175.8(5)

[a] Average value.

effect and the B_1 stretching, which does not change the dipole moment in **1a–3a**, becomes IR-active in **4a**. In the case of the small $BSiH_3$ ligand, the molecule adopts a linear geometry and the band vibration becomes again inactive. The second band of intermediate strength was assigned to CO_{ax} stretching. Its blue shift from ~1980 to 2014 cm^{-1}, comparing $[(CO)_5CrBNR_2]$ with $[(CO)_5CrBSiR_3]$, is a result of the stronger Cr→B π-backbonding present in the latter compound. The largest discrepancy observed in CO frequencies between **5a** and **5b**,**c** is a result of using significantly smaller phosphines in the model compounds, which results in very different geometries of the carbonyl groups.

Due to the small HOMO–LUMO gap in transition-metal complexes, the precise calculations of secondary properties of such compounds still remains a challenge for quantum-mechanical software. Nevertheless, the chemical shifts are reproduced with usable accuracy. Both ^{11}B and ^{13}C NMR shifts for most of the computed molecules were found to be 5–10 ppm high-field shifted with respect to the experimental values. As both experimental scales are about 250 ppm wide, the relative errors are less than 4% and the results of these computations are a valuable help for the assignment of experimental spectra. In particular, the computations reproduce properly the extreme low-field shift in the ^{11}B NMR caused by the exchange of the amino substituent with the hypersilyl group.

Bonding analysis: To gain deeper insight into the nature of bonding in borylene complexes, we examined their molecular orbitals and performed both population and topological analyses. The presented bonding analysis is based on the Natural Bond Orbitals procedure of Weinhold,[38] and, as every population analysis, is to some extent arbitrary, we have analyzed the canonical orbitals as well.

To simplify the discussion, but not to oversimplify the chemical model, we present numerical results only for the SiH_3-substituted molecules (**1–5b**). For the same reason, only pictures of the MO's of the parent molecules (**1c**, **4c**) are presented. The results for the trimethylsilyl-substituted and the parent molecules can be requested from the authors.

To gain deeper insight into the characterization of the bonding situation in the series of the compounds **1–5**, we calculated the instantaneous interaction energies (ΔE_{int}) between the metal fragment and the different ligands. In contrast to the bond dissociation energy (D_0), ΔE_{int} does not take into account any geometric relaxation, and is computed between two components with frozen geometry of the final product, that is, it is computationally less expensive. As shown by

Table 2. Selected experimental and calculated (in italics) spectroscopic data of $[(OC)_5M{=}B{=}NR_2]$ (M = Cr, Mo, W, **1–3**; R = $SiMe_3$, SiH_3, H, **a–c**), $[(OC)_5Cr{=}B\text{-}SiR_3]$ (R = $SiMe_3$, SiH_3, H; **4a–c**), $[(R'_3P)(OC)_4Cr{=}B{=}NR_2]$ (R = $SiMe_3$, R′ = Cy, **5a**; R = SiH_3, R′ = Me, **5b**; R = R′ = H, **5c**) and $[(Cy_3P)(OC)_4M{=}B{=}N(SiMe_3)_2]$ (M = Mo, **6a**; W, **7a**).

	$\tilde{\nu}$ (CO) [cm^{-1}][a]	$\delta(^{11}B)$ [ppm]	δ ($^{13}C_{ax}$) [ppm]	$\delta(^{13}C_{eq})$ [ppm][c]
1a	1942, 1981, 2064	92.3	218.0	217.6
	1949; *1980*; *2066*	*85.4*	*211.7*	*211.5*
1b	*1964*; *1991*; *2053*	*82.6*	*210.5*	*209.0*
1c	*1969*; *1995*; *2057*	*90.6*	*211.0*	*208.5*
2a	1946, 1978, 2073	89.7	206.8	207.7
	1950; *1977*; *2074*	*82.2*	*201.9*	*201.9*
2b	*1964*; *1990*; *2082*	*78.7*	*200.3*	*199.9*
2c	*1968*; *1994*; *2085*	*86.5*	*201.2*	*199.7*
3a	1941, 1967, 2075	86.6	196.5	197.2
	1944; *1971*; *2052*	*78.4*	*199.5*	*198.3*
3b	*1958*; *1982*; *2060*	*75.1*	*198.0*	*196.6*
3c	*1962*; *1988*; *2063*	*82.2*	*199.2*	*196.5*
4a	1952, 1982, 2014, 2066	204.3	213.3	213.3
	1958; *1975*; *2000*; *2047*	*208.6*	*212.2*	*208.1*
4b	*1977*; *1992*; *2015*; *2059*	*194.1*	*210.5*	*205.8*
4c	*1982*; *1995*; *2020*[b]; *2065*	*194.6*	*209.6*	*205.0*
5a	1868, 1898	93.7	–	224.3
5b	*1923*; *1924*	*83.0*	–	*212.2*
5c	*1936*; *1938*	*83.3*	–	*210.7*
6a	1894, 1912	92.0	–	213.6
7a	1887, 1903	90.0	–	205.4

[a] Computed frequencies were scaled with 0.96. [b] IR inactive vibration. [c] Average value for computed shifts.

Willock for cationic diyl complexes $-\Delta E_{int}$ closely matches D_0 ($\Delta = 3$–6 kJ).[15h]

Substitution of the chromium atom by its heavier congeners in the aminoborylene complexes leads to a larger value of $-\Delta E_{int}$ for the M–B bond ($-\Delta E_{int} = 67.7$, 69.5, and 75.2 kJ mol^{-1} for **1b**–**3b**, respectively). The 3d orbitals of chromium are the first orbitals of this symmetry and therefore they can penetrate deeper into the core region. Because of the similarity of the radii of the 3s,p and 3d orbitals, an overlapping of the ligand orbitals with 3d metal-centered orbitals leads to repulsion with the inert shell. The orthogonality of the 4d and 3d orbitals causes an increase of the radius of the 4d orbitals when changing to molybdenum. The spatial separation of the 4s,p and the 4d orbitals is bigger and thus, the repulsion is smaller, and the relativistic contraction additionally amplifies this effect in the case of tungsten. Hence, the M–B interaction energies increase in the series Cr < Mo < W.

The computational data for $[(OC)_5Cr{=}B{=}N(SiH_3)_2]$ (**1b**), $[(OC)_5Cr{=}B{-}Si(SiH_3)_3]$ (**4b**), and $[(Me_3P)(OC)_4Cr{=}B{=}N(SiH_3)_2]$ (**5b**) are shown in Table 3. The comparison of the interaction energy between the metal–carbonyl fragments and the different borylenes clearly indicates differences in the bonding situation. The lowest value of -89.4 kJ mol^{-1} for **4b** indicates, that the boron atom, which is electronically not stabilized through π-interaction by the silicon atom, creates a stronger bond with the metal than in both aminoborylene complexes. Exchange of the silyl by an amino substituent leads to a more potent sharing of the electrons with the nitrogen atom and a weakening of the Cr–B bond, hence less electron density is released from the chromium to the boron atom and therefore stronger Cr–CO interactions result. As expected, this effect is more pronounced for the axial ligand. The difference in ΔE_{int} for equatorial $Cr{-}CO_{eq}$ bonds is only ~0.4 kJ mol^{-1}, whereas in the axial $Cr{-}CO_{ax}$ bond an increase to 6.1 kJ mol^{-1} is observed. The direct influence of the *trans* ligands on the Cr→B π-backbonding can be observed in the case of **1b** and **5b**. The phosphine has very weak π-acceptor properties, thus chromium in **5b** can donate more of its electron density into the empty p orbitals of the remaining ligands, which results in considerable lower interaction energies of the B–Cr bond and also lowers ΔE_{int} for the equatorial carbonyls. The Charge Decomposition Analysis, which can be seen as quantification of the Dewar–Chatt–Duncanson model, also supports this model. The rest term q[s] (not shown in Table 3) computed for all three analyzed molecules was close to zero, thus, according to earlier reports by Frenking, these compounds can be described as donor–acceptor complexes.[41] The ratio of donation and backdonation charges (q[d] and q[b]) in **4b** is much smaller than in both aminoborylene complexes. This indicates stronger π-backdonation, however, even in this molecule σ-donation plays a dominant role, which is also reflected by the covalent bond orders: the highest Wiberg Bond Index (WBI) of the Cr–B bond is found for **4b** (0.97) and the lowest for **1b** (0.74). The phosphine-substituted complex shows an average value of 0.85. Values of the WBI below unity may seem surprising, as π-backbonding is characteristic of multiple bonds. However, the comparison with Cr–C or even B–N bonds shows that all of these values are in the range of 0.4–1.0, which is due to the polarity of all respective bonds. The natural charge of the chromium atom (−1.45) is much lower than these of the terminal atoms in the ligands, hence suggesting a strong ionic character of the metal–ligand linkage.

Table 3. Analysis of bonding in $[(OC)_5Cr{=}B{=}N(SiH_3)_2]$ (**1b**), $[(OC)_5Cr{=}B\text{-}Si(SiH_3)_3]$ (**4b**), and $[(Me_3P)(OC)_4Cr{=}B{=}N(SiH_3)_2]$ (**5b**).

	1b	**4b**	**5b**
$-\Delta E_{int}$ [kJ mol^{-1}]			
Cr–B	67.7	89.4	72.5
$Cr{-}L_{ax}$[a]	42.4	36.3	36.7
$Cr{-}CO_{eq}$[b]	45.2	44.8	46.4
charge decomposition analysis B–X[a]			
q[d]	0.791	0.529	0.876
q[b]	0.265	0.343	0.353
Wiberg bond index			
B–X	1.06	1.02	1.02
Cr–B	0.74	0.97	0.85
$Cr{-}L_{ax}$[a]	0.66	0.56	0.38
$Cr{-}CO_{eq}$[b]	0.75	0.73	0.79
natural charge			
Cr	−1.45	−1.42	−1.47
B	0.84	0.27	0.85
N/Si	−1.57	−0.12	−1.57
boron character in B–Cr [%]			
NLMO			
σ	53.7	51.2	52.2
π	–	11.2	–
π	–	11.2	–
ELF basin population and σ^2			
B–X[a]	3.52	2.17	3.53
	(1.51)	(0.96)	(1.52)
Cr–B	1.22	2.51	1.32
	(0.86)	(1.44)	(0.93)
	1.23		1.29
	(0.87)		(0.92)
$Cr{-}L_{ax}$	1.42	2.79	2.13
	(0.93)	(1.29)	(1.14)
	1.43		
	(0.95)		
$Cr{-}CO_{eq}$[b]	2.86	2.82	2.91
	(1.38)	(1.37)	(1.40)

[a] L = CO, PMe_3; X = $N(SiH_3)_2$, $Si(SiH_3)_3$. [b] Average value.

The optimal Lewis structures for aminoborylenes **1b** and **5b** and the silylborylene **4b**, given by the NBO partitioning scheme, display Cr–B single bonds, and a Cr≡B triple bond, respectively. For **1b** no reasonable structure with a Cr=B double bond could be found or defined with the CHOOSE options of the NBO program. Subsequent efforts led to a very low occupied orbital (0.42 e$^-$). The structures with a Cr–B single bond feature even less populated lone pairs (**1b**: 0.24 e$^-$; **5b**: 0.27 e$^-$) with the correct symmetry for π-type bonds with the chromium atom. The σ-type orbitals possess an equal contribution from both atoms, and both π orbitals in **4b** are dominated by chromium. Relatively high non-Lewis occupancies for **1b**, **4b** and **5b** (3.3, 2.4 and 2.7%) indicate, that these molecules are at the border line for the localized bond model, and hence, we also analyzed

the canonical orbitals of the parent compounds **1c** and **4c**. Examination of the molecular orbitals reveals that the B–Cr bond is characterized by the σ-type HOMO−3 orbital and two π-type interactions. Relevant orbitals are shown in Figure 5. In both molecules **1c** and **4c** the HOMO−3 orbitals have similar contributions from both boron and chromium atoms with a larger polarization of boron (B: 47 and 36% versus Cr: 25 and 30% for **1c** and **4c**, respectively). However, the hybridization of the boron atom differs: in **1c** a sp_z hybrid is employed and in **4c** predominantly the p_z orbital is employed. The π-type orbitals use only p_x or p_y orbitals on boron and accordingly, d_{xz} or d_{yz} orbitals on chromium with more pronounced contributions of the latter. There is a big difference between **1c** and **4c** when comparing both pairs of π orbitals (**1c**: HOMO, HOMO−2; **4c**:HOMO−1, HOMO−2), in the case of **4c** both orbitals are almost degenerate, but for **1c** the HOMO has a much smaller contribution from boron than the HOMO−2, because the p_x orbital of boron is mainly used to create a B=N π bond (HOMO−4). Therefore these calculations tend to support a model with Cr=B double-bond character in the aminoborylene and Cr≡B triple-bond character in the silylborylene complexes. The arbitrary nature of orbital localization procedures in delocalized systems like the borylene complexes discussed here, hampers a localized description of the bonding situation (see above). To avoid disadvantages of partitioning schemes based on molecular orbitals, functions like the Electron Localization Function (ELF) or Laplacian of the electron density can be used. The ELF function indicates the ratio of the local Pauli repulsion in comparison to the uniform electron gas of the same density as in the examined system.[42] The ELF values are normalized in the range of 0–1 and they are close to 1 in regions of core shells, covalent bonds, and lone pairs.

The most obvious difference in the topology of ELF when comparing amino- and silylborylenes is the existence of two disynaptic valence basins V(B,Cr) in **1b** and **5b**, with their attractors positioned in the $BNSi_2$ plane, whereas only one such basin is found in **4b** (see Table 3 and Figure 6). The latter one displays almost an axial symmetry and, as found for $[(CO)_5CrBF]$, features a ring attractor.[43] The population N of the B–Cr valence basins of all three molecules is similar and amounts up to about 10% less than this of Cr–C bonds. The difference in the ELF topology of the three borylene complexes leads to a discrepancy in the population analysis of the basins. In particular, as there are cross contributions between both V(B,Cr) basins in **1b** and **5b**, their variances $\sigma^2(N)$ with values of ~0.9 differ significantly from 1.44 found for **4b**. However, as both former basins are mutually bound, they can be considered as one basin (i.e., they can be concatenated with disregard of cross contributions), and then, the analysis gives results (**1b**: Cr–B $N=2.45$ $\sigma^2=1.22$; **5b**: $N=2.61$, $\sigma^2=1.39$) similar to those of **4b**.

Similarly high values of the population variances ($\sigma^2 > 1.3$) and relative fluctuations $\lambda(\lambda=\sigma^2/N \geq 0.5)$, which arise from adjacent basins, were reported to be sensible criteria of electron delocalization, for example, in aromatic systems.[44] In the case of the aforementioned complexes, the corresponding adjacent basins comprise the core basins of Cr with the largest contribution (ca. 36%), the B–X valence basin (14%; X=$N(SiH_3)_2$, $Si(SiH_3)_3$), and the four Cr–C valence basins (8% each). Both borylene complexes with a higher π-backdonation, that is, **4b** and **5b**, have a slightly increased contribution from the core basin C(Cr) and smaller ones from the V(B–X) basins in comparison to the aminoborylene complex **1b**. All of these results deriving from ELF calculations indicate, like the aforementioned partitioning schemes, a rather delocalized bonding situation for terminal borylene complexes, which is only insufficiently expressed by simple Lewis formulae. In addition, we considered the σ- and π-type orbitals contribution to the Cr–B basins as a parameter for the Cr→B backdonation. The lowest π-fraction (20%) was found for the aminoborylene complex **1b**, followed by its phosphine substituted analogue

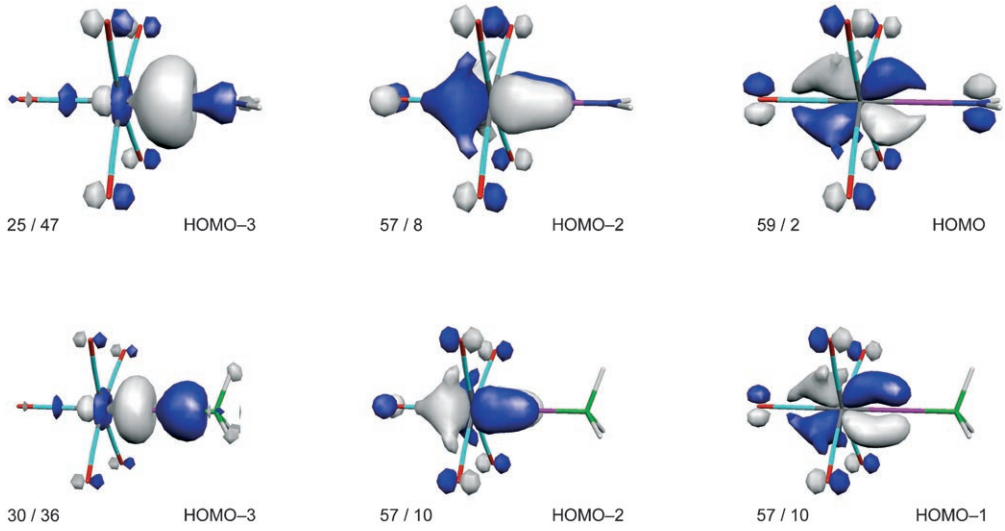

Figure 5. Kohn–Sham orbitals of σ- and π-components in **1c** (top) and **4c** (bottom). Contributions of chromium and boron atomic orbitals are given (in%).

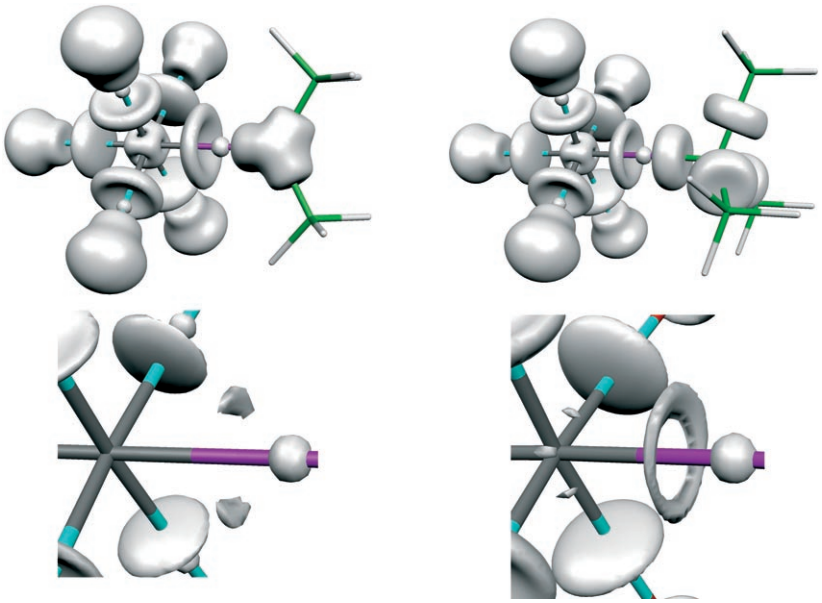

Figure 6. Isosurfaces ELF = 0.75 in **1b** (left) and **4b** (right) with detailed view of the Cr/B region for higher ELF values (0.87). The envelopes around the SiH_3 groups are omitted for clarity.

5b (35%), whereas the silylborylene complex **4b** displays the highest π-contribution (50%), thus again emphasizing the higher Cr–B multiple bond character in the latter complex.

Conclusion

Salt elimination reactions between dianionic transition metal carbonylates and dihaloboranes have been employed for the synthesis of a range of terminal borylene complexes. The bulky, albeit rather electrophilic aminoborane $Cl_2BN(SiMe_3)_2$ yielded the complete series of Group 6 aminoborylene complexes $[(OC)_5M{=}B{=}N(SiMe_3)_2]$ (M = Cr, **1a**; Mo, **2a**; W, **3a**). Attempts to establish a corresponding series of hypersilylborylene complexes, yielded the chromium complex $[(OC)_5Cr{=}B{-}Si(SiMe_3)_3]$ (**4a**), but failed for the heavier Group 6 elements. Corresponding reactions of $Br_2BN(SiMe_3)_2$ with $Na_2[Fe(CO)_4]$ provided spectroscopic evidence for the formation of the target iron–aminoborylene complex, $[(OC)_4Fe{=}B{=}N(SiMe_3)_2]$ (**8**), which was, however, accompanied by the novel ferracyclopentadiene complex, $[Fe_2\{\mu\text{-}C_2O_2(BN(SiMe_3)_2)\}_2(CO)_6]$ (**9**). These results indicate that salt elimination constitutes a valuable method for the synthesis of borylene complexes, but is to be restricted to certain combinations of dihaloboranes and dianionic carbonylates. The reactivity of the compounds $[(OC)_5M{=}B{=}N(SiMe_3)_2]$ (M = Cr, **1a**; Mo, **2a**; W, **3a**) towards photochemically induced CO–phosphine exchange was examined, yielding a corresponding series of phosphine–borylene complexes *trans*-$[(Cy_3P)(OC)_4M{=}B{=}N(SiMe_3)_2]$ (M = Cr, **5a**; Mo, **6a**;W, **7a**).

The results of DFT calculations performed on suitable model complexes of **1a**–**5a** together with a comparison of structural data provided insight into the nature of the metal–boron bond of terminal borylene complexes. In particular, the extent of metal–boron interaction depends on the transition metal (W > Mo > Cr), the π-acceptor abilities of the ligand in *trans*-position to the borylene ($R_3P{-}Cr$ > $OC{-}Cr$) and the proportion of π-stabilization provided by the boron bound substituent ($R_3Si{-}B$ > $R_2N{-}B$).

Experimental Section

All manipulations were performed either under dry argon or in vacuo using standard Schlenk line and glovebox techniques. Solvents (toluene and hexane) were purified by distillation under dry argon from appropriate drying agents (sodium and sodium wire, respectively) and stored under the same inert gas over molecular sieves. IR spectra were recorded as toluene solutions between KBr plates on either a Perkin–Elmer FTIR 1720X or Bruker Vector 22 FTIR spectrometer. NMR spectra were acquired on either a Varian Unity 500 (^{1}H: 499.834; ^{11}B: 160.364; ^{13}C: 125.697 MHz) or Bruker Avance 500 (^{1}H: 500.133; ^{11}B: 160.472; ^{13}C: 125.777 MHz) NMR spectrometer. ^{1}H and $^{13}C\{^1H\}$ NMR spectra were referenced to external TMS via the residual protio solvent (^{1}H) or the solvent itself (^{13}C). $^{11}B\{^1H\}$ NMR spectra were referenced to external $BF_3{\cdot}OEt_2$ and $^{31}P\{^1H\}$ NMR spectra to 85% H_3PO_4. Microanalyses for C, H and N were performed on either a Carlo Erba model 1106 or a Leco CHNS-932 Elemental Analyzer. $Na_2[M(CO)_5]$ (M = Cr, Mo, W),[45] $K_2[Fe(CO)_4]$,[46] $X_2BN(SiMe_3)_2$ (X = Cl, Br)[47] and $Cl_2BSi(SiMe_3)_3$[48] were prepared according to the literature.

Compound 2a: A suspension of $Na_2[Mo(CO)_5]$ (4.78 mmol) in toluene (10 mL) was cooled to ca. −80 °C. $Cl_2BN(SiMe_3)_2$ (1.16 g, 4.78 mmol) was then added dropwise to the rapidly stirred suspension. The reaction mixture was subsequently allowed to warm to room temperature and stirred for a further ca. 16 h. All volatiles were then removed in vacuo from the resulting cloudy, brown solution, giving a brown solid. Recrystallization from hexane at −65 °C afforded pure **2a** (0.59 g, 31%) as colorless crystals. ^{1}H NMR (500 MHz, C_6D_6, 25 °C, TMS): $\delta = 0.15$ ppm (s, $SiMe_3$); $^{11}B\{^1H\}$ NMR (160 MHz, C_6D_6, 25 °C, $Et_2O{\cdot}BF_3$): $\delta = 89.7$ ppm; $^{13}C\{^1H\}$ NMR (126 MHz, C_6D_6, 25 °C, TMS): $\delta = 3.4$ ($SiMe_3$), 206.8 (CO_{ax}), 207.7 ppm (CO_{eq}); IR (toluene): $\tilde{\nu} = 2071$(w), 1982(m), 1945(vs) cm^{-1} (CO); elemental analysis calcd (%) for $C_{11}H_{18}MoNBO_5Si_2$ (407.9): C 32.45, H 4.46, N 3.44; found: C 32.42, H 4.25, N 3.18.

Compound 5a: A yellow solution of **1a** (0.030 g, 0.083 mmol) and PCy_3 (0.023 g, 0.083 mmol) in C_6D_6 (0.6 mL) was photolyzed at room temperature in a quartz NMR tube for 5 h. After that the solvent of the pale yellow reaction mixture was evaporated in vacuo. The oily residue was dissolved in hexane (2 mL) and stored at −30 °C. After 6 d pale yellow crystals of **5a** had formed (0.031 g, 61%). ^{1}H NMR (400 MHz, C_6D_6, 21 °C, TMS): $\delta = 2.04$–1.53 (m, 33H, Cy), 0.38 ppm (s, 18H, $SiMe_3$); $^{13}C\{^1H\}$ NMR (101 MHz, C_6D_6, 21 °C, TMS): $\delta = 224.3$ (d, ^2J(C,P) = 13 Hz, CO), 37.3 (d, ^1J(C,P) = 13 Hz, C_1, Cy), 29.9 (s, $C_{3,5}$, Cy), 28.1 (d, ^2J(C,P) = 10 Hz, $C_{2,6}$, Cy), 26.8 (s, C_4, Cy), 3.0 ppm (s, $SiMe_3$); $^{11}B\{^1H\}$ NMR (96 MHz C_6D_6, 23 °C, $Et_2O{\cdot}BF_3$): $\delta = 94$ ppm (brs); $^{31}P\{^1H\}$ NMR (162 MHz, C_6D_6, 21 °C, H_3PO_4): $\delta = 64.7$ ppm (s); IR (toluene): $\tilde{\nu} = 1898$, 1868 cm^{-1} (CO); elemental analysis calcd (%) for

$C_{28}H_{51}NBCrO_4PSi_2$ (615.7): C 54.62, H 8.35, N 2.28; found: C 54.65, H 8.04, N 2.30.

Compound 6a: A yellow solution of **2a** (0.030 g, 0.074 mmol) and PCy_3 (0.021 g, 0.074 mmol) in C_6D_6 (0.1 mL) and THF (0.5 mL) was photolyzed at room temperature in a quartz NMR tube for 3 h. The solvent of the pale yellow reaction mixture was evaporated in vacuo. The oily residue was dissolved in hexane (2 mL) and stored at −30 °C. After 1 day pale yellow solid of **6a** had formed (0.028 g, 57 %). ^{1}H NMR (500 MHz, C_6D_6, 25 °C, TMS): δ = 2.10–1.10 (m, 33 H, Cy), 0.37 ppm (s, 18 H, $SiMe_3$); ^{13}C{^{1}H} NMR (126 MHz, C_6D_6, 25 °C, TMS): δ = 213.6 (d, ^2J(C,P) = 9 Hz, CO), 36.6 (d, ^1J(C,P) = 11 Hz, C_1, Cy), 30.5 (d, ^3J(C,P) = 1 Hz, $C_{3,5}$, Cy), 28.0 (d, ^2J(C,P) = 10 Hz, $C_{2,6}$, Cy), 26.8 (s, C_4, Cy), 3.3 ppm (s, $SiMe_3$); ^{11}B{^{1}H} NMR (160 MHz, C_6D_6, 25 °C, $Et_2O{\cdot}BF_3$): δ = 92 ppm (brs); ^{31}P{^{1}H} NMR (202 MHz, C_6D_6, 25 °C, H_3PO_4): δ = 51.1 ppm (s); IR (toluene): $\tilde{\nu}$ = 1912, 1894 cm^{-1} (CO); elemental analysis calcd (%) for $C_{28}H_{51}NBMoO_4PSi_2$ (659.6): C 50.99, H 7.79, N 2.12; found: C 51.12, H 7.36, N 2.01.

Compound 7a: A yellow solution of **3a** (0.030 g, 0.061 mmol) and PCy_3 (0.017 g, 0.061 mmol) in C_6D_6 (0.1 mL) and THF (0.5 mL) was photolyzed at room temperature in a quartz NMR tube for 3 h. After that the solvent of the pale brown reaction mixture was evaporated in vacuo. The oily residue was dissolved in hexane (2 mL) and stored at −30 °C. After 2 d pale brown solid of **7a** had formed (0.025 g, 55 %). ^{1}H NMR (500 MHz, C_6D_6, 24 °C, TMS): δ = 2.10–1.10 (m, 33 H, Cy), 0.38 ppm (s, 18 H, $SiMe_3$); ^{13}C{^{1}H} NMR (126 MHz, C_6D_6, 24 °C, TMS): δ = 205.4 (d, ^2J(C,P) = 7 Hz, CO), 37.5 (d, ^1J(C,P) = 15 Hz, C_1, Cy), 30.7 (s, $C_{3,5}$, Cy), 27.9 (d, ^2J(C,P) = 10 Hz, $C_{2,6}$, Cy), 26.8 (d, ^4J(C,P) = 1 Hz, C_4, Cy), 3.3 ppm (s, $SiMe_3$); ^{11}B{^{1}H} NMR (160 MHz, C_6D_6, 24 °C, $Et_2O{\cdot}BF_3$): δ = 90 ppm (brs); ^{31}P{^{1}H} NMR (202 MHz, C_6D_6, 24 °C, H_3PO_4): δ = 35.0 ppm (s, ^1J(P,W) = 219 Hz); IR (toluene): $\tilde{\nu}$ = 1903, 1887 cm^{-1} (CO); elemental analysis calcd (%) for $C_{28}H_{51}NBO_4PSi_2W$ (747.5): C 44.99, H 6.88, N 1.87; found: C 45.30, H 6.48, N 1.77.

Compound 8: A suspension of $K_2[Fe(CO)_4]$ (1.05 g, 4.25 mmol) in toluene (15 mL) was prepared in a grease-free Schlenk tube. $Br_2BN(SiMe_3)_2$ (1.33 g, 4.04 mmol) was then added, the reaction mixture frozen, the vessel evacuated and CO (1 atm) admitted. After thawing, the suspension was treated in an ultrasonic bath for 3 d. All volatiles were then removed from the resulting cloudy, brown solution to afford a brown residue. The solid was subsequently suspended in hexane (10 mL) and the insoluble residue separated by centrifugation. The supernatant liquors were then decanted and all volatiles removed in vacuo to afford **8** as a dark brown oil (0.38 g, 28 %). ^{1}H NMR (500 MHz, C_6D_6, 25 °C, TMS): δ = 0.11 ppm (s, 18 H, $SiMe_3$); ^{11}B{^{1}H} NMR (160 MHz, C_6D_6, 25 °C, $Et_2O{\cdot}BF_3$): δ = 87.3 ppm (brs); ^{13}C{^{1}H} NMR (126 MHz, C_6D_6, 25 °C, TMS): δ = 1.4 ($SiMe_3$), 233.4 ppm (CO); IR (toluene): $\tilde{\nu}$ = 2056(s), 2032(m), 1986(s) 1941(s) cm^{-1} (CO).

Compound 9: A suspension of $K_2[Fe(CO)_4]$ (0.83 g, 3.39 mmol) in toluene (15 mL) was prepared in a grease-free Schlenk tube and $Cl_2BN(SiMe_3)_2$ (0.78 g, 3.22 mmol) added. The colorless reaction mixture was then treated in an ultrasonic bath for 3 d. All volatiles were subsequently removed from the resulting cloudy, dark brown solution in vacuo to afford a dark brown residue. Hexane (10 mL) was added and the insoluble material separated by centrifugation. The supernatant liquors were then decanted and stored at −65 °C. After 1 d, the bright yellow crystals of pure **9** (0.12 g, 5 %) that had formed were isolated and dried in vacuo. ^{1}H NMR (500 MHz, C_6D_6, 25 °C, TMS): δ = 0.23 (s, 18 H, $SiMe_3$), 0.43 ppm (s, 18 H, $SiMe_3$); ^{11}B{^{1}H} NMR (160 MHz, C_6D_6, 25 °C, $Et_2O{\cdot}BF_3$): δ = 27.3 ppm (brs); ^{13}C{^{1}H} NMR (126 MHz, C_6D_6, 25 °C, TMS): δ = 3.4 ($SiMe_3$), 4.0 ($SiMe_3$) 129.8 (Fe*C*O), 182.9 (Fe*C*O), 210.1 (CO), 211.2 ppm (CO); IR (toluene): $\tilde{\nu}$ = 2078(w), 2036(vs), 2012(s) 1995(m) cm^{-1} (CO); elemental analysis calcd (%) for $C_{22}H_{36}N_2B_2Fe_2O_{10}Si_4$ (734.2): C 35.99, H 4.94, N 3.82; found: C 35.61, H 4.74, N 3.53.

Crystal structure determination: The crystal data of **2a**, **5a**, **6a**, and **9** were collected on a Bruker Apex diffractometer with CCD area detector and graphite monochromated $Mo_{K\alpha}$ radiation, and that of **7a** were collected on a Bruker X8Apex diffractometer with CCD area detector and multi-layer mirror monochromated $Mo_{K\alpha}$ radiation. The structures were solved using direct methods, refined with the Shelx software package (G. Sheldrick, University of Göttingen 1997) and expanded using Fourier techniques. All non-hydrogen atoms were refined anisotropically. Hydrogen atoms were assigned idealized positions and were included in structure factor calculations. The crystals of **6a**, **7a** and **9**, respectively, were non-merohedrical twins arising from 180° rotation about the reciprocal axis 0 0 1. Integration was performed for two domains and an absorption correction was done with the twinabs program. Refinement against HKLF5 formatted F^2 gave BASF = 0.28, 0.35, and 0.026.

Crystal data for **2a**: $C_{11}H_{18}BMoNO_5Si_2$, M_r = 407.19, yellow blocks, 0.26 × 0.22 × 0.20, triclinic space group $P\bar{1}$, a = 9.291(3), b = 9.347(3), c = 12.168(4) Å, α = 109.560(5), β = 98.618(5), γ = 101.551(5)°, V = 948.3(5) Å^3, Z = 2, ρ_{calcd} = 1.426 g cm^{-3}, μ = 0.832 cm^{-1}, $F(000)$ = 412, T = 173(2) K, R_1 = 0.0165, wR_2 = 0.0424, 3765 independent reflections $2\theta \leq$ 52.14° and 190 parameters.

Crystal data for **5a**: $C_{28}H_{51}BCrNO_4PSi_2$, M_r = 615.66, yellow blocks, 0.25 × 0.16 × 0.10, monoclinic space group $P2_1/c$, a = 20.8563(14), b = 9.1712(6), c = 18.3901(12) Å, β = 100.7070(10)°, V = 3456.4(4) Å^3, Z = 4, ρ_{calcd} = 1.183 g cm^{-3}, μ = 0.477 cm^{-1}, $F(000)$ = 1320, T = 193(2) K, R_1 = 0.0417, wR_2 = 0.1074, 6830 independent reflections $2\theta \leq$ 52.12° and 343 parameters.

Crystal data for **6a**: $C_{28}H_{51}BMoNO_4PSi_2$, M_r = 659.60, colorless blocks, 0.26 × 0.22 × 0.20, triclinic space group $P\bar{1}$, a = 9.5468(7), b = 10.5124(7), c = 17.6163(12) Å, α = 80.788(2), β = 80.620(2), γ = 86.7140(18)°, V = 1720.9(2) Å^3, Z = 2, ρ_{calcd} = 1.273 g cm^{-3}, μ = 0.528 cm^{-1}, $F(000)$ = 696, T = 100(2) K, R_1 = 0.0428, wR_2 = 0.0869, 9864 independent reflections $2\theta \leq$ 52.9° and 344 parameters.

Crystal data for **7a**: $C_{28}H_{51}BNO_4PSi_2W$, M_r = 747.51, colorless blocks, 0.22 × 0.165 × 0.11, triclinic space group $P\bar{1}$, a = 9.5178(6), b = 10.4203(7), c = 17.5192(13) Å, α = 80.735(4), β = 80.785(5), γ = 86.802(4)°, V = 1691.9(2) Å^3, Z = 2, ρ_{calcd} = 1.467 g cm^{-3}, μ = 3.563 cm^{-1}, $F(000)$ = 760, T = 100(2) K, R_1 = 0.0322, wR_2 = 0.1019, 10818 independent reflections $2\theta \leq$ 53.14° and 344 parameters.

Crystal data for **9**: $C_{22}H_{36}B_2Fe_2N_2O_{10}Si_4$, M_r = 601.97, orange bars, 0.21 × 0.18 × 0.10, monoclinic space group $P2_1/m$, a = 6.496(4), b = 29.640(16), c = 9.167(5) Å, β = 93.813(7)°, V = 1761.2(16) Å^3, Z = 2, ρ_{calcd} = 1.135 g cm^{-3}, μ = 1.374 cm^{-1}, $F(000)$ = 624, T = 173(2) K, R_1 = 0.0500, wR_2 = 0.1141, 2932 independent reflections $2\theta \leq$ 53° and 200 parameters.

CCDC–624816, -624818, -624820, -624819, -624817 contain the supplementary crystallographic data for this paper. These data can be obtained free of charge from The Cambridge Crystallographic Data Centre via www.ccdc.cam.ac.uk/data_request/cif.

[1] For current examples see: a) Y. Chauvin, *Angew. Chem.* **2006**, *118*, 3824–3831; *Angew. Chem. Int. Ed.* **2006**, *45*, 3740–3747; b) R. R. Schrock, *Angew. Chem.* **2006**, *118*, 3832–3844; *Angew. Chem. Int. Ed.* **2006**, *45*, 3748–3759; c) R. H. Grubbs, *Angew. Chem.* **2006**, *118*, 3845–3850; *Angew. Chem. Int. Ed.* **2006**, *45*, 3760–3765.

[2] M. Scholl, S. Ding, C. W. Lee, R. H. Grubbs, *Org. Lett.* **1999**, *1*, 953–956.

[3] K. H. Döth, H. Fischer, P. Hofmann, F. R. Kreissl, U. Schubert, K. Weiss, *Transition Metal Carbene Complexes*, Verlag Chemie, Weinheim, **1983**.

[4] a) H. Braunschweig, *Angew. Chem.* **1998**, *110*, 1882–1898; *Angew. Chem. Int. Ed.* **1998**, *37*, 1786–1801; b) H. Braunschweig, M. Colling, *Coord. Chem. Rev.* **2001**, *223*, 1–51; c) H. Braunschweig, M. Colling, *Eur. J. Inorg. Chem.* **2003**, 393–403; d) H. Braunschweig, *Adv. Organomet. Chem.* **2004**, *51*, 163–192; e) H. Braunschweig, C. Kollann, D. Rais, *Angew. Chem.* **2006**, *118*, 5389–5400; *Angew. Chem. Int. Ed.* **2006**, *45*, 5254–5274.

[5] H. Braunschweig, M. Colling, C. Hu, K. Radacki, *Angew. Chem.* **2003**, *115*, 215–218; *Angew. Chem. Int. Ed.* **2003**, *42*, 205–208.

[6] a) H. Braunschweig, C. Kollann, U. Englert, *Angew. Chem.* **1998**, *110*, 3355–3357; *Angew. Chem. Int. Ed.* **1998**, *37*, 3179–3180; b) H. Braunschweig, M. Colling, C. Kollann, H. G. Stammler, B. Neumann, *Angew. Chem.* **2001**, *113*, 2359–2361; *Angew. Chem. Int. Ed.* **2001**, *40*, 2298–2300.

[7] H. Braunschweig, M. Colling, C. Kollann, K. Merz, K. Radacki, *Angew. Chem.* **2001**, *113*, 4327–4329; *Angew. Chem. Int. Ed.* **2001**, *40*, 4198–4200.
[8] D. L. Coombs, S. Aldridge, C. Jones, D. J. Willock, *J. Am. Chem. Soc.* **2003**, *125*, 6356–6357.
[9] D. L. Kays (nee Coombs), J. K. Day, L.-L. Ooi, S. Aldridge, *Angew. Chem.* **2005**, *117*, 7623–7626; *Angew. Chem. Int. Ed.* **2005**, *44*, 7457–7460.
[10] S. Aldridge, C. Jones, T. Gans-Eichler, A. Stasch, D. L. Kays (née Coombs), N. D. Coombs, D. J. Willock, *Angew. Chem.* **2006**, *118*, 6264–6268; *Angew. Chem. Int. Ed.* **2006**, *45*, 6118–6122.
[11] H. Braunschweig, K. Radacki, D. Scheschkewitz, G. R. Whitell, *Angew. Chem.* **2005**, *117*, 1685–1688; *Angew. Chem. Int. Ed.* **2005**, *44*, 1658–1660.
[12] a) F. M. Bickelhaupt, U. Radius, A. W. Ehlers, R. Hoffmann, E. J. Baerends, *New J. Chem.* **1998**, *22*, 1–3; b) A. W. Ehlers, E. J. Baerends, F. M. Bickelhaupt, U. Radius, *Chem. Eur. J.* **1998**, *4*, 210–221; c) U. Radius, F. M. Bickelhaupt, A. W. Ehlers, N. Goldberg, R. Hoffmann, *Inorg. Chem.* **1998**, *37*, 1080–1090.
[13] H. Braunschweig, T. Wagner, *Angew. Chem.* **1995**, *107*, 904–905; *Angew. Chem. Int. Ed. Engl.* **1995**, *34*, 825–826.
[14] J. Su, X.-W. Li, R. C. Crittendon, C. F. Campana, G. H. Robinson, *Organometallics* **1997**, *16*, 4511–4513.
[15] a) C. Boehme, G. Frenking, *Chem. Eur. J.* **1999**, *5*, 2184–2189; b) C. L. B. MacDonald, A. H. Cowley, *J. Am. Chem. Soc.* **1999**, *121*, 12113–12126; c) J. Uddin, C. Boehme, G. Frenking, *Organometallics* **2000**, *19*, 571–582; d) C. Boehme, J. Uddin, G. Frenking, *Coord. Chem. Rev.* **2000**, *197*, 249–276; e) Y. Chen, G. Frenking, *J. Chem. Soc. Dalton Trans.* **2001**, 434–440; f) J. Uddin, G. Frenking, *J. Am. Chem. Soc.* **2001**, *123*, 1683–1693; g) T. Bollwein, P. J. Brothers, H. L. Hermann, P. Schwertfeger, *Organometallics* **2002**, *21*, 5236–5242; h) S. Aldridge, A. Rossin, D. L. Coombs, D. J. Willock, *Dalton Trans.* **2004**, 2649–2654.
[16] B. Wrackmeyer, *Angew. Chem.* **1999**, *111*, 817–818; *Angew. Chem. Int. Ed.* **1999**, *38*, 771–772.
[17] a) H. Braunschweig, B. Ganter, *J. Organomet. Chem.* **1997**, *545–546*, 163–167; b) H. Braunschweig, M. Koster, *J. Organomet. Chem.* **1999**, *588*, 231–234; c) H. Braunschweig, C. Burschka, M. Burzler, S. Metz, K. Radacki, *Angew. Chem.* **2006**, *118*, 4458–4461; *Angew. Chem. Int. Ed.* **2006**, *45*, 4352–4355.
[18] N. P. Rath, T. P. Fehlner, *J. Am. Chem. Soc.* **1988**, *110*, 5345–5349.
[19] H. Braunschweig, D. Rais, *Heteroat. Chem.* **2005**, *16*, 566–571.
[20] H. Braunschweig, M. Colling, C. Kollann, U. Englert, *J. Chem. Soc. Dalton Trans.* **2002**, 2289–2296.
[21] a) H. Braunschweig, M. Forster, K. Radacki, *Angew. Chem.* **2006**, *118*, 2187–2189; *Angew. Chem. Int. Ed.* **2006**, *45*, 2132–2134; b) H. Braunschweig, T. Herbst, D. Rais, F. Seeler, *Angew. Chem.* **2005**, *117*, 7627–7629; *Angew. Chem. Int. Ed.* **2005**, *44*, 7461–7463.
[22] a) H. Braunschweig, D. Rais, K. Uttinger, *Angew. Chem.* **2005**, *117*, 3829–3832; *Angew. Chem. Int. Ed.* **2005**, *44*, 3763–3766; b) H. Braunschweig, K. Radacki, D. Rais, K. Uttinger, *Organometallics* **2006**, *25*, 5159–5164.
[23] a) H. Braunschweig, M. Koster, K. W. Klinkhammer, *Angew. Chem.* **1999**, *111*, 2368–2370; *Angew. Chem. Int. Ed.* **1999**, *38*, 2229–2231; b) H. Braunschweig, K. W. Klinkhammer, M. Koster, K. Radacki, *Chem. Eur. J.* **2003**, *9*, 1303–1309.
[24] a) H. Braunschweig, B. Ganter, M. Koster, T. Wagner, *Chem. Ber.* **1996**, *129*, 1099–1101; b) H. Braunschweig, M. Koster, R. Wang, *Inorg. Chem.* **1999**, *38*, 415–416.
[25] M. J. Bennett, W. A. G. Graham, R. A. Smith, R. P. Stewart, Jr., *J. Am. Chem. Soc.* **1973**, *95*, 1684–1686.
[26] H. Nöth, Nuclear Magnetic Resonance Spectroscopy of Boron Compounds, Springer Verlag, **1978**.
[27] E. A. V. Ebsworth, D. W. H. Rankin, S. Cradock, *Structural Methods in Inorganic Chemistry*, 2nd ed., Blackwell, Oxford, **1991**, p. 227.
[28] a) C. A. Mirkin, K.-L. Lu, G. L. Geoffroy, A. L. Rheingold, *J. Am. Chem. Soc.* **1990**, *112*, 461–462; b) T. E. Snead, C. A. Mirkin, K.-L. Lu, S.-B. T. Nguyen, W.-C. Feng, H. L. Beckman, G. L. Geoffroy, A. L. Rheingold, B. S. Haggerty, *Organometallics* **1992**, *11*, 2613–2622.
[29] W. P. Fehlhammer, H. Stolzenberg in *Comprehensive Organometallic Chemistry, Vol. 1* (Eds.: G. Wilkinson, F. G. A. Stone), Pergamon, Oxford, **1982**, p. 548–555.
[30] M. Casarin, D. Ajò, G. Granozzi, E. Tondello, S. Aime, *Inorg. Chem.* **1985**, *24*, 1241–1246.
[31] Gaussian03, Revision B.04, M. J. Frisch, G. W. Trucks, H. B. Schlegel, G. E. Scuseria, M. A. Robb, J. R. Cheeseman, J. A. Montgomery, Jr., T. Vreven, K. N. Kudin, J. C. Burant, J. M. Millam, S. S. Iyengar, J. Tomasi, V. Barone, B. Mennucci, M. Cossi, G. Scalmani, N. Rega, G. A. Petersson, H. Nakatsuji, M. Hada, M. Ehara, K. Toyota, R. Fukuda, J. Hasegawa, M. Ishida, T. Nakajima, Y. Honda, O. Kitao, H. Nakai, M. Klene, X. Li, J. E. Knox, H. P. Hratchian, J. B. Cross, C. Adamo, J. Jaramillo, R. Gomperts, R. E. Stratmann, O. Yazyev, A. J. Austin, R. Cammi, C. Pomelli, J. W. Ochterski, P. Y. Ayala, K. Morokuma, G. A. Voth, P. Salvador, J. J. Dannenberg, V. G. Zakrzewski, S. Dapprich, A. D. Daniels, M. C. Strain, O. Farkas, D. K. Malick, A. D. Rabuck, K. Raghavachari, J. B. Foresman, J. V. Ortiz, Q. Cui, A. G. Baboul, S. Clifford, J. Cioslowski, B. B. Stefanov, G. Liu, A. Liashenko, P. Piskorz, I. Komaromi, R. L. Martin, D. J. Fox, T. Keith, M. A. Al-Laham, C. Y. Peng, A. Nanayakkara, M. Challacombe, P. M. W. Gill, B. Johnson, W. Chen, M. W. Wong, C. Gonzalez, J. A. Pople, Gaussian, Inc., Pittsburgh PA, **2003**.
[32] A. D. Becke, *J. Chem. Phys.* **1993**, *98*, 5648–5652.
[33] S. H. Vosko, L. Wilk, M. Nusair, *Can. J. Phys.* **1980**, *58*, 1200.
[34] C. Lee, W. Yang, R. G. Parr, *Phys. Rev. B* **1988**, *37*, 785–789.
[35] Wachters+f and Stuttgart RSC 1997 ECP Basis Sets were obtained from the Extensible Computational Chemistry Environment Basis Set Database, Version 02/25/04, as developed and distributed by the Molecular Science Computing Facility, Environmental and Molecular Sciences Laboratory which is part of the Pacific Northwest Laboratory, PO Box 999, Richland, Washington 9935 (USA), and funded by the US Department of Energy.
[36] R. E. Stratmann, J. C. Burant, G. E. Scuseria, M. J. Frisch, *J. Chem. Phys.* **1997**, *106*, 10175–10183.
[37] TOPMOD package, S. Noury, X. Krokidis, F. Fuster, B. Silvi, Universite Pierre et Marie Curie, **1997**.
[38] NBO5.0, E. D. Glendening, J. K. Badenhoop, A. E. Reed, J. E. Carpenter, J. A. Bohmann, C. M. Morales, F. Weinhold, Theoretical Institute, University of Wisconsin, Madison, **2001**.
[39] S. Dapprich, G. Franking, *J. Phys. Chem.* **1995**, *99*, 9352–9362.
[40] MOLEKEL 4.0, P. Flükiger, H. P. Lüthi, S. Portmann, J. Weber, Swiss Center for Scientific Computing, Manno (Switzerland), **2000**.
[41] S. F. Vyboishchikiv, G. Frenking, *Chem. Eur. J.* **1998**, *4*, 1428–1438.
[42] M. Kohout, F. R. Wagner, Y. Grin, *Theor. Chem. Acc.* **2002**, *108*, 150–156.
[43] For comparison we calculated $[(OC)_5CrBF]$, which is isoselectronic to $[(OC)_6Cr]$. The valence basin V(B,Cr) of the ELF surface has the form of a ring.
[44] A. Savin, B. Silvi, F. Coionna, *Can. J. Chem.* **1996**, *74*, 1088–1096.
[45] J. M. Maher, R. P. Beatty, N. J. Cooper, *Organometallics* **1985**, *4*, 1354–1361.
[46] J. A. Gladysz, W. Tam, *J. Org. Chem.* **1978**, *43*, 2279–2280.
[47] W. Haubold, U. Kraatz, *Z. Anorg. Allg. Chem.* **1976**, *421*, 105–110.
[48] C. Kollann, PhD thesis, RWTH Aachen, Germany, **1999**.

Received: October 25, 2006
Published online: March 15, 2007

